Available online at www.sciencedirect.com
SCIENCE DIRECT®
Thermochimica Acta 413 (2004) 31–38
thermochimica acta
www.elsevier.com/locate/tca

Thermal behavior and thermal decomposition study of porphyrin polymers containing different spacer groups

Chunxiu Guan [a], liqing Li [a], Donghua Chen [a,*], Zongyong Gao [b], Wenbo Sun [b]

[a] *College of Chem and Life Science, South-Central University for Nationalities, Wuhan 430074, Hubei, China*
[b] *Hubei Institute of Chemistry, Wuhan 430074, Hubei, China*

Received 27 September 2003; received in revised form 6 November 2003; accepted 6 November 2003

Abstract

A series of porphyrin polymers containing different spacer groups was synthesized and studied using TG, DSC and FTIR. The thermal behaviors including the possible conformation transition and phase transition of porphyrins were studied during the heating process at lower temperature. Polymers with spacer groups exhibit higher thermal stability compared to that without spacer group. Activation energies obtained by the iterative isoconversion method gave support to this observation. The phenomenological, kinetic and mechanistic aspects of thermal decomposition of these porphyrin polymers have been also studied. It is very interesting that all the decomposition courses of porphyrin polymers follow the same mechanism function "Avrami-Erofeev equation".

Keywords: Thermal stability; Decomposition; Dynamic TG; Kinetic; Porphyrins

1. Introduction

Porphyrins serve as functional group have enormous potential for applications including those in catalysis of organic reactions [1], magnetic resonance imaging [2] and optoelectronics technique [3–5]. Porphyrin macrocycles are very flexible for being π-delocalized system and by introducing substituents selectively at the β- or *meso*-positions, changing the central metal or extending the macrocycle, the molecule can be decorated for many practical applications. All these properties make porphyrins fit for the molecule design of the nonlinear-optical materials [6,7], which can be tuned at will for the photoelectron technology application. To the best of our knowledge, at present, most work of porphyrin compound focus on the preparation technique and synthesis route. However, little is known on the thermal and kinetic studies of such material, which are very important information to application of these porphyrins. In view of this, we reported here the thermal behavior and thermal decomposition kinetic study of the porphyrin polymers containing different spacer groups prepared by condensation polymerization. We use the differential scanning calorimetry technology and FTIR spectrum to confirm the existence of the possible conformation transition or the phase transition of these three polymers during heating process at lower temperature. The decomposition process and kinetic analysis using dynamic TG method of these samples have also been described in detail.

2. Experimental

2.1. Material

The three samples: 1,4-benzylene as spacer porphyrin polymer (PPI), *meso*,*meso*-linked porphyrin polymer (PPII), methylene bridge-linked porphyrin polymer (PPIII) were prepared by condensation polymerization at Hubei Institute of Chemistry. Their structures were given in Scheme 1, which have been characterized by MS, ^{1}H NMR, ^{13}C NMR and FTIR.

2.2. Measurement of differential scanning calorimetry (DSC) and FTIR spectra

The physical changes observed during the heating process of these polymers were measured by DSC and FTIR. The

* Correspondence author. Tel.: +86-27-87496844; fax: +86-27-87532752.
E-mail address: chendh46@sina.com (D. Chen).

0040-6031/$ – see front matter © 2003 Elsevier B.V. All rights reserved.
doi:10.1016/j.tca.2003.11.002

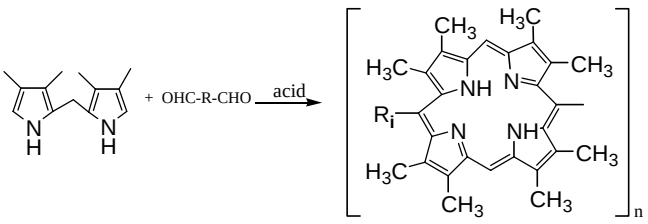

Scheme 1. The structures of the three porphyrin polymers.

DSC analysis was performed on a METTLER-TOLEDO DSC822e (Co., Switzerland). The temperature was recorded from room temperature to 120 °C with heating rates of 5 °C min^{-1} under the nitrogen flow of about 50 ml min^{-1}. The reference pan was pure aluminum pan. The temperature and energy of instruments had been calibrated by standard In before all measurements. The infra-red spectra (NICOLET-NEXUS 470, Co., USA) were recorded for samples of PPI, PPII and PPIII at the given temperatures.

2.3. Thermogravimetry (TG) and derivative thermogravimetry (DTG)

Dynamic TG of polymer powders was conducted on a TGS-2 thermal-balance (Perkin-Elmer Co., USA). The nominal heating rates of 5, 10, 15, 20 and 25 °C min^{-1} were employed from room temperature to 950 °C. A pure nitrogen flow of 80 ml min^{-1} was used with sample size ranging from 1.50 to 2.50 mg.

3. Kinetics analysis

3.1. Calculation of activation energy E_a

Thermal decomposition of solid-state material is subjected to general Eq. (1):

$$\frac{d\alpha}{dT} = \frac{1}{\beta} A e^{-E_a/RT} f(\alpha) \quad (1)$$

where $\beta = dT/dt$ is the heating rate. In most experiments, the heating rate is kept constant. From Eq. (1), KAS equation [8,9] is deduced.KAS equation:

$$\ln\frac{\beta}{T^2} = \ln\left[\frac{AE_a}{g(\alpha)R}\right] - \frac{E_a}{RT} \quad (2)$$

Iterative procedure is used to approach the exact value of E_a, the equation is [10]:

$$\ln\frac{\beta}{h(x)T^2} = \ln\left[\frac{AE_a}{g(\alpha)R}\right] - \frac{E_a}{RT} \quad (3)$$

The iterative procedure is as follows:

(i) Supposing $h(x) = 1$ to estimate the initial value of the activation energy E_{a1}. The conventional isoconversional method stops calculating at this step.
(ii) Using E_{a1} to calculate $h(x)$, then from Eq. (3) to calculate a new value E_{a2} for the activation energy from the plot of $\ln[\beta/h(x)T^2]$ versus $1/T$.
(iii) Repeating step2, replacing E_{a1} with E_{a2}.When $E_{ai} - E_{ai-1} < 0.01$ kJ mol^{-1}, the last value E_{ai} is the exact value of activation energy of the reaction.

3.2. Determination of the most probable mechanism function

The classical Achar equation [11] and Coats–Redfern equation [12] were introduced to determination of the most probable mechanism function of the decompositions. Typical 31 kinds of kinetic models in the thermal decomposition [13] were applied in these two equations, respectively. Comparing the kinetic parameters obtained from these two methods, the probable kinetic model differential form $f(\alpha)$ or integral form $g(\alpha)$ may be selected, which the values of activation energies are close to each other with better correlation coefficients and also are close to the values obtained by the iterative procedure from KAS equation.

From Eq. (1), Eq. (4) is derived at maximum reaction rate [14].

$$-\frac{1}{d f(\alpha)/d\alpha} = -\frac{1}{f'(\alpha_{max})} = \frac{A}{\beta}\frac{RT_{max}^2}{E_a}\exp\left(-\frac{E_a}{RT_{max}}\right) \quad (4)$$

The subscript "max" denotes the variables at the maximum reaction rate. Then, combining Eq. (4) with Eq. (5) gives

$$g(\alpha) = \int_0^a \frac{d\alpha}{f(\alpha)} = \frac{A}{\beta}\int_0^T e^{-E_a/RT}\,dT = \frac{AEe^{-x}}{\beta R x^2}h(x) \quad (5)$$

$$g(\alpha_{max}) \times f'(\alpha_{max}) = -h\left(\frac{E_a}{RT_{max}}\right) \quad (6)$$

Eq. (6) indicates that α_{max} value depends only on E_a/RT_{max} value for a definite kinetic model. This quantitative relation can be applied to estimate the limits of α_{max} for various kinetic models and then classify them by the magnitude of α_{max}.

4. Results and discussion

4.1. Thermal behavior of the porphyrins at lower temperature

4.1.1. DSC observations

The information of the thermal behavior at lower temperature was obtained by DSC with the heating rate of 5 °C min^{-1}. On heating the three samples respectively, a

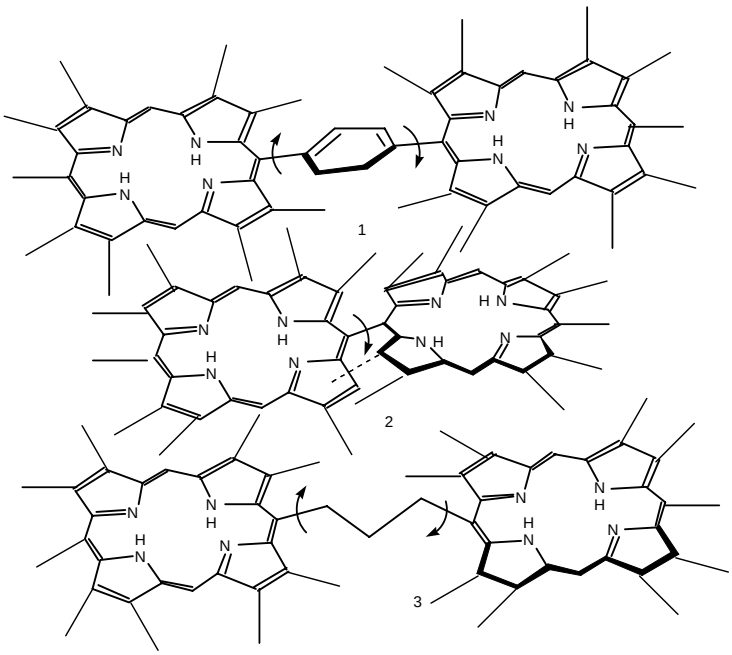

Fig. 1. Geometry of the porphyrins and the possible rotations and oscillations about the bonds in these dimers: (1) PPI; (2) PPII; and (3) PPIII.

weak endothermic peak was observed at 72.1 °C (ΔH = 18.74 J g^{-1}), 93.4 °C (ΔH = 9.75 J g^{-1}) and 73.4 °C (ΔH = 64.62 J g^{-1}). All the temperatures here represent the values of extrapolated onsets of the curves of DSC. The enthalpies (ΔH) are the thermodynamics parameter of these temperature variation processes, which were estimated from each DSC peak area computed by standard procedure in DSC apparatus, respectively.

The successful removal of traces of solvent by a heat treatment at 70 °C could be controlled by the TG signal that did not show any mass change. Therefore, the endothermal peaks could clearly be attributed to phase transformations within the porphyrin polymer samples. By considering the various intramolecular motions possible for the porphyrin polymers [15], it is reasonable to assume that this behavior is due to restricted rotation(s) and/or oscillation(s) about the bonds (Fig. 1). Similarly, since porphyrins usually have high melting points, the dominant processes involved in the fusion at the lower temperature must involve the hydrocarbon chains [16].

On cooling from the given temperature, nothing was observed in the DSC curves for PPI and PPIII. But an exothermic peak was observed at 93.2 °C (ΔH = −7.66 J g^{-1}) in the DSC curve for PPII.

Upon reheating these samples, an endothermic peak observed at 91.3 °C in the DSC curves for PPII, similar to that observed on the first heating. These physical changes are shown in Figs. 2–4.

4.1.2. Infra-red spectra

Infra-red spectra were recorded for the samples of porphyrin polymers at various temperatures between 70–100 °C. There were no changes observed in the FTIR

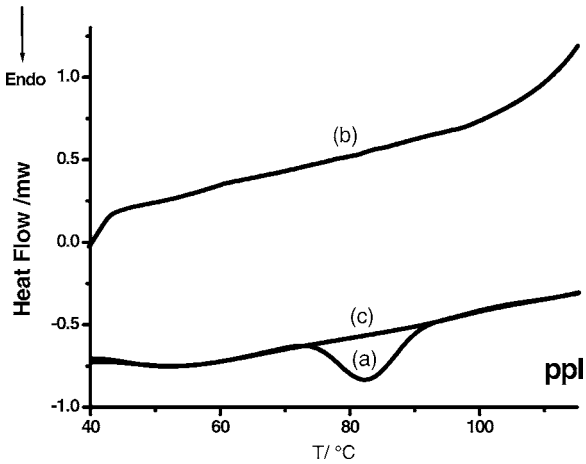

Fig. 2. DSC curves for PPI: (a) initial heating; (b) cooling; and (c) reheating the same sample (heating rate/cooling rate: 5 °C min^{-1}).

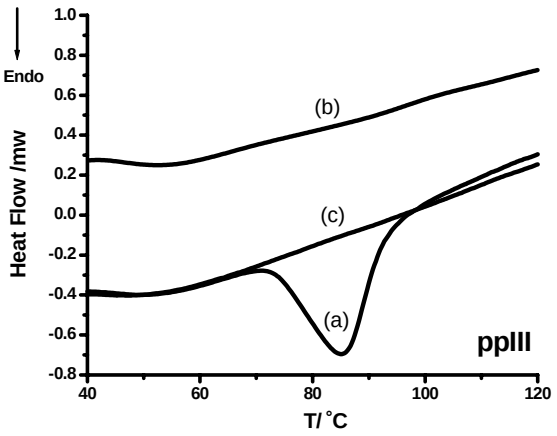

Fig. 3. DSC curves for PPIII: (a) initial heating; (b) cooling; and (c) reheating the same sample (heating rate/cooling rate: 5 °C min^{-1}).

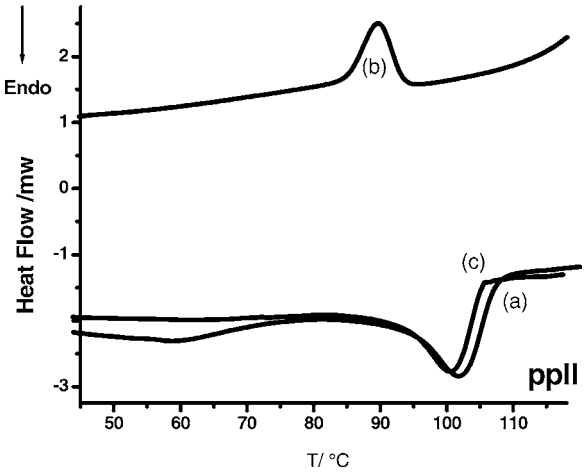

Fig. 4. DSC curves for PPII: (a) initial heating; (b) cooling; and (c) reheating the same sample (heating rate/cooling rate: 5 °C min^{-1}).

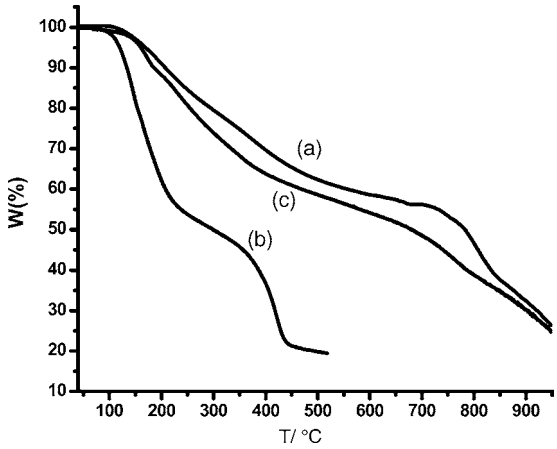

Fig. 6. Dynamic TG curves for (a) PPI, (b) PPII, and (c) PPIII with heating rate was 10 °C min^{-1} in nitrogen.

spectra for PPI and PPIII but PPII, from which we can see that there were not any changes of the structure and components of PPI and PPIII. Typical spectra of PPII are shown in Fig. 5.

From Fig. 5, it can be obtained that in the solid at 75 °C, the N–H stretching vibration is observed at 3316 cm^{-1}, close to that reported for porphyrins [16]. On heating this shows only a slight decrease in energy, suggesting that no major changes in PPII structure occur during this process. However, marked changes occur in the bands in the 2850–2940 cm^{-1} region. These are associated mainly with C–H stretching vibrations of the undecyl chains [17], and show changes in both intensity and band width on going from solid to liquid phase. The ratio of the intensity of the bands in vibrational spectra at 2920 and 2856 cm^{-1}, assigned to the antisymmetric and symmetric C–H stretching vibrations, has been shown to be a good measure of the conformational disorder and lateral packing of alkane chains [17].

Two conclusions can be drawn from these observations above. Firstly, the observed physical changes of PPI and PPIII on heating procedure at lower temperature were figured the possible conformation transition. Secondly, the differences observed in the DSC behavior of PPII show that, in agreement with the infra-spectra observations, a phase change happens during the heating process.

4.2. Thermal decomposition process of porphyrin polymers

Figs. 6 and 7 show the dynamic TG plots in nitrogen atmosphere of the three polymers at a heating rate of 10 K min^{-1} and the typical TG, DTG curves for the scanning sample PPII. The phenomenological aspects of the porphyrin polymers are presented in Table 1.

We used TG technique to speculate on the probable decomposition process of the three porphyrin polymers. The 1,4-benzylene as spacer porphyrin polymer (PPI) undergoes decomposition in two-stages. The observed mass loss (42.13%) of the first decomposition stage may be attributed to the decomposition of half a macrocyclic of PPI (the theoretical value of 42.17%). The corresponding mass loss

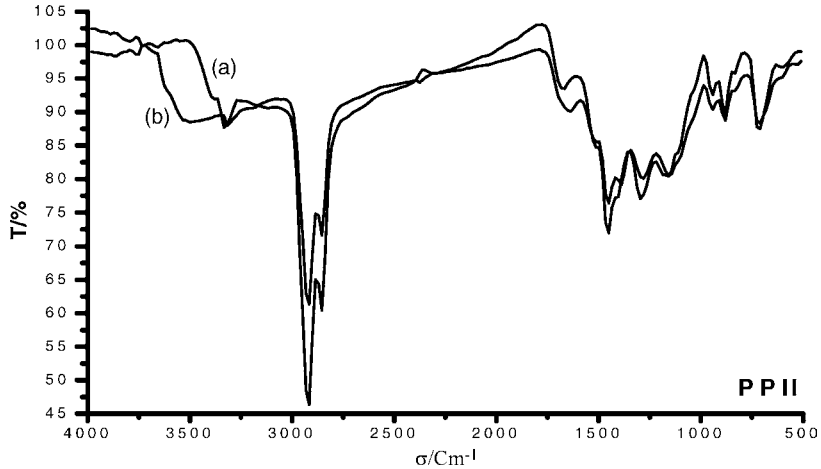

Fig. 5. FTIR spectra observed for PPII at: (a) 75 °C and (b) 100 °C.

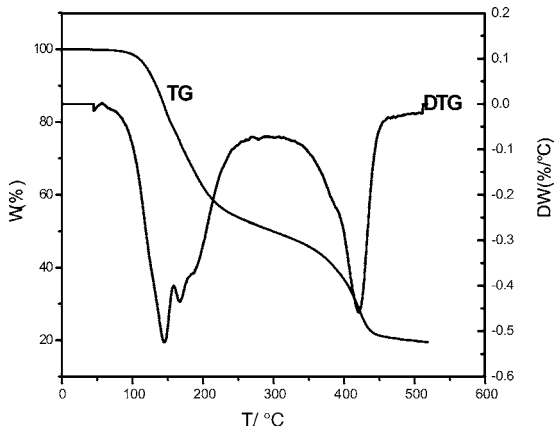

Fig. 7. Typical TG, DTG curves for PPII with heating rate of 10 °C min^{-1} in nitrogen.

(15.97%) of the second stage is due to the broken of benzene ring from the other half of the macrocyclic (the theoretical value of 15.67%).

The *meso*,*meso*-linked porphyrin polymer (PPII) undergoes decomposition in two-stages. The observed mass loss (49.57%) of the first stage may be attributed to the decomposition of half a macrocyclic of PPII (the theoretical value of 50.00%). The corresponding mass loss (25.52%) of the second stage is likely to the decomposition of half part from the other half macrocyclic (the theoretical value of 25.00%).

The methylene bridge-linked porphyrin polymer (PPIII) undergoes decomposition in two-stages. The first stage is probable the decomposition of methylene chain (the theoretical value of 9.09%), which different from the first decomposition stage of PPI. The second stage starts at 195 °C and is a continuous one. The steady mass loss observed in this stage may be due to the disintegration of the macrocyclic of PPIII successively.

From the structures of these three porphyrin polymers, it can be seen that the conjugative effect created from the benzene with the porphyrin ring exists in the system of PPI, which don't exists in the systems of PPII and PPIII. This conjugative effect increases the thermal stability of the polymer and also makes the bond energy of the benzene with the porphyrin ring lager than that of the porphyrin ring itself. That being so PPI has the better thermal stability than PPII and PPIII.

4.3. Thermal decomposition kinetics of porphyrin polymers

4.3.1. Kinetic parameters

All the well-defined stages were selected for the study of the kinetics of decomposition of the porphyrin polymers. As mentioned in Section 3, the kinetic parameters (the activation energy E_a and the pre-exponential factor A) were calculated using the iterative procedure from KAS equation and the Coats–Redfern equation. The typical values of E_a for the two decomposition steps of PPII at the rate of 10 °C min^{-1} corresponding to different values of α are shown in Table 2.

The entropy of activation ΔS can be calculated using the equation

$$A = \frac{kT_S}{h} e^{\Delta S/R} \quad (7)$$

where k is the Boltzmann constant, h the Planck's constant, and T_S the peak temperature.

The various kinetic parameters calculated are given in Table 8. The activation energies E_a in the different stages are in the range of 41.19–147.04 kJ mol^{-1}. The respective values of the pre-exponential factor A vary from 3.29×10^3 to 6.12×10^7 s^{-1}. The corresponding values of the entropy of activation ΔS are in the range -180.41 to -99.71 J mol^{-1}. The negative values of entropy of activation indicate that the activated complex has a more order structure than the reactants [18].

4.3.2. Kinetic mechanism function

The kinetic parameters were calculated by the classic integral and differential method. Furthermore, when the 'real' kinetic model is determined, the activation energies obtained from iterative method will conform to that obtained from Achar equation and Coats–Redfern equation with better correlation coefficients. It is very interesting that all the decomposition courses of porphyrin polymers are following the same mechanism function "$g(a) = [-\ln(1-a)]^{1/m}$" with different values of m. Hence the mechanism is "random nucleation and growth" representing "Avrami-Erofeev equation". The possible kinetic models and respective kinetic parameters from differential and integral equations at various heating rates for PPI, PPII, PPIII are shown in Tables 3–8. It is not difficult to find that the results obtained by using the method we proposed have the uniqueness.

Table 1
Phenomenological data for the thermal decomposition of PPI, PPII and PPIII ($\beta = 10$ °C min^{-1})

Samples	Stage of decomposition	TG plateaux (°C)	DTG peak (°C)	T_d (°C/10%)	Mass loss (calculated, %)
PPI	I	110–634	202	161	42.13 (42.17)
	II	754–858	808	770	15.97 (15.67)
PPII	I	101–251	146	123	49.57 (50.00)
	II	287–458	422	361	25.52 (25.00)
PPIII	I	102–193	173	130	10.65 (9.09)
	II	Continuous	–	–	–

Table 2
The activation energies for the two decomposition steps of PPII at the rate of 10 °C min^{-1} by using KAS method and iterative procedure

Conversion degree (α)	E_a (kJ mol^{-1}) for step I		E_a (kJ mol^{-1}) for step II	
	KAS method	$\ln[\beta/h(x)T^2] \sim 1/T$	KAS method	$\ln[\beta/h(x)T^2] \sim 1/T$
0.1	49.88	50.21	109.94	110.37
0.2	47.86	48.23	126.25	126.64
0.3	46.40	46.80	133.64	134.02
0.4	43.90	44.35	143.32	143.69
0.5	43.69	44.16	146.30	146.65
0.6	44.23	44.72	148.53	148.91
0.7	46.10	46.59	145.10	145.49
0.8	48.61	49.13	145.72	146.08
0.9	40.52	41.19	141.67	142.07
Average	45.69	46.15	137.83	138.21

Table 3
The kinetic parameters from differential method and integral method at the five heating rates for the first decomposition step of PPI

β (K min^{-1})	Function number	Coats–Redfern equation			Achar equation		
		E_a (kJ mol^{-1})	$\ln A$ (s^{-1})	R	E_a (kJ mol^{-1})	$\ln A$ (s^{-1})	R
5	29	137.41	11.55	0.9954	129.61	9.49	0.9958
10	29	137.46	11.97	0.9953	127.30	9.88	0.9961
15	29	145.98	14.17	0.9945	133.37	12.27	0.9943
20	29	139.21	13.66	0.9952	137.78	11.82	0.9955
25	29	147.90	14.19	0.9935	140.09	12.07	0.9945

Table 4
The kinetic parameters from differential method and integral method at the five heating rates for the second decomposition step of PPI

β (K min^{-1})	Function number	Coats–Redfern equation			Achar equation		
		E_a (kJ mol^{-1})	$\ln A$ (s^{-1})	R	E_a (kJ mol^{-1})	$\ln A$ (s^{-1})	R
5	9	165.09	12.56	0.9986	134.33	9.05	0.9909
10	9	165.95	12.26	0.9989	139.33	9.44	0.9309
15	9	168.33	12.72	0.9972	154.44	11.39	0.9549
20	9	148.39	9.50	0.9971	144.83	10.55	0.9932
25	9	141.03	9.68	0.9969	115.87	7.16	0.9703

Table 5
The kinetic parameters from differential method and integral method at the five heating rates for the first decomposition step of PPII

β (K min^{-1})	Function number	Coats–Redfern equation			Achar equation		
		E_a (kJ mol^{-1})	$\ln A$ (s^{-1})	R	E_a (kJ mol^{-1})	$\ln A$ (s^{-1})	R
5	7	50.13	8.92	0.9977	40.30	5.46	0.9863
10	7	49.36	8.10	0.9933	33.69	3.05	0.9895
15	7	55.30	10.51	0.9984	45.98	7.40	0.9862
20	7	47.38	8.18	0.9939	35.84	4.34	0.9601
25	7	53.33	9.80	0.9985	44.09	6.70	0.9833

Table 6
The kinetic parameters from differential method and integral method at the five heating rates for the second decomposition step of PPII

β (K min^{-1})	Function number	Coats–Redfern equation			Achar equation		
		E_a (kJ mol^{-1})	$\ln A$ (s^{-1})	R	E_a (kJ mol^{-1})	$\ln A$ (s^{-1})	R
5	9	159.06	21.48	0.9986	144.15	18.87	0.9801
10	9	127.78	15.85	0.9986	132.84	16.87	0.9867
15	9	133.84	16.96	0.9975	134.72	17.23	0.9840
20	9	122.78	15.08	0.9980	135.33	17.36	0.9963
25	9	156.85	14.43	0.9970	133.48	17.04	0.9920

Table 7
The kinetic parameters from differential method and integral method at the five heating rates for the first decomposition step of PPIII

β (K min^{-1})	Function number	Coats–Redfern equation			Achar equation		
		E_a (kJ mol^{-1})	ln A (s^{-1})	R	E_a (kJ mol^{-1})	ln A (s^{-1})	R
5	8	70.53	13.00	0.9991	61.89	10.61	0.9994
10	8	65.16	11.61	0.9989	58.82	10.78	0.9990
15	8	61.39	11.26	0.9990	57.51	9.48	0.9978
20	8	71.39	13.28	0.9998	71.62	13.43	0.9982
25	8	55.75	10.15	0.9992	66.04	12.14	0.9933

Table 8
Kinetic parameters for the thermal decompositions of the porphyrin polymers

Samples	Stage of decomposition	E_a (kJ mol^{-1})	A (s^{-1})	ΔS (J mol^{-1})	Function number	Mechanism
PPI	I	125.02	6.12×10^7	−99.71	29	Avrami-Erofeev equation ($m = 1/4$)
	II	147.04	2.11×10^6	−134.55	9	Avrami-Erofeev equation ($m = 2$)
PPII	I	46.15	3.29×10^3	−180.41	7	Avrami-Erofeev equation ($m = 1$)
	II	138.21	7.65×10^6	−120.17	9	Avrami-Erofeev equation ($m = 2$)
PPIII	I	67.98	1.10×10^5	−151.75	8	Avrami-Erofeev equation ($m = 3/2$)

Table 9
The theoretical limits of α_{max} of solid state reactions in the basic models

Model	α_{max}
A_2	0.612–0.627
A_3	0.619–0.629
A_4	0.622–0.630
R_3	0.669–0.696
D_3	0.629–0.687
R_2	0.720–0.743
D_4	0.715–0.763
D_2	0.783–0.823

The quantitative relation in Eq. (6) can be applied to estimate the limits of a_{max} for various kinetic models and then classify them by the magnitude of $a_{max.}$ The limits of a_{max} thus calculated are listed in Table 9. It is seen that the basic models are classified into four groups. Then we used this method to verify the mechanism functions we obtained above.

The values of a_{max} for the different decomposition processes of PPI, PPII, PPIII at five heating rates are shown in Table 10.

From Table 10, we can see that almost the values we calculated are in the range of limits of α_{max} for Am model. Then, the results from two different methods have the uniformity.

Table 10
The calculated limits of α_{max} of decomposition reactions

β	α_{max}				
	PPI step I	PPI step II	PPII step I	PPII step II	PPIII step I
5	0.628	0.616	0.599	0.638	0.619
10	0.612	0.601	0.609	0.662	0.607
15	0.659	0.602	0.618	0.602	0.624
20	0.601	0.615	0.596	0.626	0.655
25	0.625	0.625	0.607	0.601	0.621

4.4. Thermal stability

From the decomposition temperatures and the values of activation energies in Tables 1 and 8, the information of thermal stability of the porphyrin polymers containing different spacer groups can be obtained that the spacer group in the porphyrin polymers will influence their thermal stability. The porphyrin polymers containing spacer groups have better thermal stability than that without spacer group. And the conjugative effect of spacer group on the porphyrin ring will increase their thermal stability and make the broken of the spacer group from the polymer uneasy. The order of thermal stability is therefore: PPI > PPIII > PPII. But the decomposition temperatures of these polymers are all not very high. So, we suggest that these porphyrin polymers should be used at lower temperature.

5. Conclusion

- Differences observed in the DSC behavior on heating the porphyrin polymers containing different spacer groups. The observed physical changes of PPI and PPIII which containing the spacer groups on heating procedure at lower temperature were figured the possible conformation transition. And, the differences observed in the DSC behavior of PPII without spacer group show that, in agreement with the infra-spectra observations, a phase change happens during the heating process.
- The thermal stability of this series of porphyrin polymers was studied using TG. It is found that the porphyrins containing spacer groups are more stable than that without spacer group. Activation energies of the decomposition steps were determined according to the iterative method from the classic KAS equation. The activation energies evaluated by this method indicate the order of thermal

stability as PPI > PPIII > PPII. It is very interesting that all the decomposition courses of porphyrin polymers are following the same mechanism function "Avrami-Erofeev equation".

Acknowledgements

This work was supported by the key natural science fund of Department of Science and Technology of Hubei Province.

References

[1] B. Meunier, Chem. Rev. 92 (1992) 1411.
[2] R.B. Lauffer, Chem. Rev. 87 (1987) 901.
[3] S.V. Rao, N.K.M.N. Srinivas, D.N. Rao, et al., Opt. Commun. 182 (2000) 255.
[4] M.J. Plater, S. Ariken, G. Bourhill, Tetrahedron 58 (2002) 2405.
[5] D.N. Rao, Opt. Mater. 21 (2002) 45.
[6] H.L. Anderson, Chem. Commun. 23 (1999) 2323.
[7] H.L. Anderson, Angew. Chem. Int. Ed. Engl. 33 (1994) 655–657.
[8] H.E. Kissinger, Anal. Chem. 29 (1957) 1702.
[9] T. Ozawa, Thermochim. Acta 203 (1992) 15.
[10] Z. Gao, M. Nakada, I. Amasaki, Thermochim. Acta 369 (2001) 137.
[11] A.W. Coats, J.P. Redern, Nature (London) 1 (1964) 68.
[12] B.N. Achar, Proc. Int. Clay Conf. 1 (1966) 67.
[13] X. Gao, D. Pollimore, Thermochim. Acta 47 (1993) 215.
[14] Z. Gao, I. Amasaki, M. Nakada, Thermochim. Acta 385 (2002) 95.
[15] D.P. Arnold, P.C. Healy, M.J. Hodgson, et al., J. Organometall. Chem. 607 (2000) 41.
[16] H.D. Burrows, A.M. Rocha Gonsalves, M.L.P. Leitao, et al., Supramol. Sci. 4 (1997) 241.
[17] I.R. Hill, I.W. Levin, J. Chem. Phys. 70 (1979) 842.
[18] M.K.M. Nair, P.K. Radhakrishnan, Themochim. Acta 261 (1995) 141–149.